

ADAPTIVE SOLUTIONS OF A STABILIZED MIXED FINITE ELEMENT METHOD FOR POROUS MEDIA EQUATIONS

Tomás P. Barrios^a, José Manuel Cascón^b and María González^c

^a*Departamento de Matemática y Física Aplicadas, Universidad Católica de la Santísima Concepción,
Alonso de Ribera 2850, Concepción, Chile, tomas@ucsc.cl.*

^b*Departamento de Economía e Historia Económica, Universidad de Salamanca, Salamanca, 37008,
Spain, casbar@usal.es.*

^c*Departamento de Matemáticas, Universidad de la Coruña, Campus de Elviña s/n, 15071, A Coruña,
Spain, maria.gonzalez.taboada@udc.es.*

Keywords: Darcy flow, mixed finite element, stabilization, a posteriori error estimator.

Abstract. Through numerical experiments, we explore the theoretical properties of an a-posteriori error estimator of an augmented mixed method applied to Darcy law. More precisely, we show numerical evidence confirming the theoretical properties of the estimator, and illustrating the capability of the corresponding adaptive algorithm to localise the singularities and boundary layers of the solutions.

1 INTRODUCTION

In the paper [Masud and Hughes \(2002\)](#), an augmented mixed finite element method applied to Darcy flow was presented and analysed. The approach there is based on the introduction of suitable least-squares terms arising from the constitutive and equilibrium equations. It is shown there that the continuous and discrete augmented formulations are well posed. In particular, the discrete scheme allows the utilization of the simple finite element spaces, such as, piecewise linear continuous elements for the velocity and pressure, which should be easily generalized to 3D.

On the other hand, assuming that physical parameters are equal to one and neglecting gravity force, it is provided in [Larson and Malqvist \(2008\)](#) a residual based a posteriori error analysis to the augmented approach developed in [Masud and Hughes \(2002\)](#). In addition, taking into account that the velocity of this phenomena really lives in the space of Lebesgue square-integrable vector fields whose divergence is also Lebesgue square-integrable ($H(\text{div}, \Omega)$), more recently in [Barrios et al. \(2014\)](#), we consider conforming finite elements, such as, Raviart-Thomas or Brezzi-Douglas-Marini elements for the velocity fields and piecewise linear continuous functions for pressure, to develop a reliable and efficient a posteriori error estimator for this kind of problem, including physical parameters, such as density, permeability, viscosity and gravity force.

The purposes of the present work are, first, to give a review of a priori and a posteriori error analysis of the augmented mixed formulation applied to porous media equations, and secondly, to show numerical evidence confirming the theoretical properties of the augmented scheme and the corresponding adaptive algorithm based on the a posteriori error estimator proposed in [Barrios et al. \(2014\)](#).

The rest of the paper is organised as follows. In Sections 2 and 3, we give a review of the a priori and a posteriori error analysis of the augmented mixed formulation. Finally, several numerical results illustrating the performance of the augmented mixed finite element scheme, and the reliability and efficiency of the a posteriori error estimator, are provided in Section 4.

2 THE AUGMENTED MIXED VARIATIONAL FORMULATION

Let Ω be a bounded domain in \mathbb{R}^d ($d = 2, 3$), with piecewise smooth boundary Γ , and denote by \mathbf{n} the unit outward normal vector to Γ . Let $\rho > 0$ be the density, \mathbf{g} the gravity vector, g_c a conversion constant, φ the volumetric flow rate source or sink, and ψ the normal component of the velocity field on the boundary. We denote $\mathbf{f} := -\frac{\rho}{g_c}\mathbf{g}$. Then, the Darcy problem reads: Find the Darcy velocity vector $\mathbf{v} : \Omega \rightarrow \mathbb{R}^d$ and the pressure $p : \Omega \rightarrow \mathbb{R}$ such that

$$\begin{cases} \mathcal{K}^{-1}\mathbf{v} + \nabla p = \mathbf{f} & \text{in } \Omega, & \text{div}(\mathbf{v}) = \varphi & \text{in } \Omega, \\ \text{and } \mathbf{v} \cdot \mathbf{n} = \psi & \text{on } \Gamma, \end{cases} \quad (1)$$

where $\mathcal{K} \in [L^\infty(\Omega)]^{d \times d}$ is a given symmetric and uniformly positive definite matrix-valued function, that is, there exists $\alpha > 0$ such that

$$\left(\mathcal{K}(\mathbf{x}) \mathbf{y} \right) \cdot \mathbf{y} \geq \alpha \|\mathbf{y}\|^2, \quad \text{a.e. } \mathbf{x} \in \Omega, \quad \forall \mathbf{y} \in \mathbb{R}^d, \quad (2)$$

Then, we also have that

$$\left(\mathcal{K}^{-1}(\mathbf{x}) \mathbf{y} \right) \cdot \mathbf{y} \geq \frac{\alpha}{\|\mathcal{K}\|^2} \|\mathbf{y}\|^2, \quad \text{a.e. } \mathbf{x} \in \Omega, \quad \forall \mathbf{y} \in \mathbb{R}^d, \quad (3)$$

and

$$\frac{1}{\|\mathcal{K}\|} \|\mathbf{y}\| \leq \|\mathcal{K}^{-1}(\mathbf{x})\mathbf{y}\|, \quad \text{a.e. } \mathbf{x} \in \Omega, \quad \forall \mathbf{y} \in \mathbb{R}^d. \quad (4)$$

In many applications it is assumed an isotropic medium, that is $\mathcal{K} = \frac{\kappa}{\mu} \mathbf{I}$, where $\kappa > 0$ and $\mu > 0$ are, respectively, the permeability and the viscosity of the porous medium, and \mathbf{I} is the identity matrix. We also assume that the data φ and ψ satisfy the compatibility constraint $\int_{\Omega} \varphi = \int_{\Gamma} \psi$.

In what follows, we introduce the spaces $L_0^2(\Omega) := \{v \in L^2(\Omega) / \int_{\Omega} v \, dx = 0\}$, $H^1(\Omega) := \{v \in L^2(\Omega) / \nabla v \in [L^2(\Omega)]^d\}$, $H(\text{div}, \Omega) := \{\mathbf{v} \in [L^2(\Omega)]^d / \text{div}(\mathbf{v}) \in L^2(\Omega)\}$, $H_{\zeta} := \{\mathbf{w} \in H(\text{div}, \Omega) : \mathbf{w} \cdot \mathbf{n} = \zeta \text{ on } \Gamma\}$ and $M := H^1(\Omega) \cap L_0^2(\Omega)$.

Let $\mathbf{H} := H(\text{div}, \Omega) \times M$ and let us denote by $\|\cdot\|_{\mathbf{H}}$ the corresponding product norm. Then, given positive parameters κ_1 and κ_2 , we consider from Barrios et al. (2014) the following augmented variational formulation for (1): Find $(\mathbf{v}, p) \in H_{\psi} \times M$ such that

$$A_s((\mathbf{v}, p), (\mathbf{w}, q)) = F_s(\mathbf{w}, q), \quad \forall (\mathbf{w}, q) \in H_0 \times M, \quad (5)$$

where the bilinear form $A_s : \mathbf{H} \times \mathbf{H} \rightarrow \mathbb{R}$ and the linear functional $F_s : \mathbf{H} \rightarrow \mathbb{R}$ are defined by

$$\begin{aligned} A_s((\mathbf{v}, p), (\mathbf{w}, q)) &:= \int_{\Omega} \mathcal{K}^{-1} \mathbf{v} \cdot \mathbf{w} - \int_{\Omega} p \, \text{div}(\mathbf{w}) + \int_{\Omega} q \, \text{div}(\mathbf{v}) \\ &+ \kappa_1 \int_{\Omega} (\nabla p + \mathcal{K}^{-1} \mathbf{v}) \cdot (\nabla q - \mathcal{K}^{-1} \mathbf{w}) + \kappa_2 \int_{\Omega} \text{div}(\mathbf{v}) \, \text{div}(\mathbf{w}), \end{aligned}$$

and

$$F_s(\mathbf{w}, q) := \int_{\Omega} \mathbf{f} \cdot \mathbf{w} + \int_{\Omega} \varphi q + \kappa_1 \int_{\Omega} \mathbf{f} \cdot (\nabla q - \mathcal{K}^{-1} \mathbf{w}) + \kappa_2 \int_{\Omega} \varphi \, \text{div}(\mathbf{w}),$$

for all $(\mathbf{v}, p), (\mathbf{w}, q) \in \mathbf{H}$. Assuming $\kappa_1 \in (0, \frac{\alpha}{\|\mathcal{K}\|^2 \|\mathcal{K}^{-1}\|^2})$ and $\kappa_2 > 0$ it is possible to prove strong ellipticity of the bilinear form $A_s(\cdot, \cdot)$ (The proof is developed in Lemma 2.1 in Barrios et al. (2014), also see Masud and Hughes (2002) and Barrios et al. (2007)). Then, the well posedness of the Problem (5), that is, existence, uniqueness and stability, follow from the classical Lax-Milgram Lemma.

In order to establish the discrete scheme, let $\{\mathcal{T}_h\}_{h>0}$ be a family of shape-regular meshes of $\bar{\Omega}$ made up of triangles in 2D or tetrahedra in 3D. We denote by h_T the diameter of an element $T \in \mathcal{T}_h$ and define $h := \max_{T \in \mathcal{T}_h} h_T$. Let H_h and M_h be any finite element subspaces of $H(\text{div}, \Omega)$ and M , respectively. Then, the Galerkin scheme associated to Problem (5) is: Find $(\mathbf{v}_h, p_h) \in (H_h \cap H_{\psi}) \times M_h$ such that

$$A_s((\mathbf{v}_h, p_h), (\mathbf{w}_h, q_h)) = F_s(\mathbf{w}_h, q_h), \quad \forall (\mathbf{w}_h, q_h) \in (H_h \cap H_0) \times M_h. \quad (6)$$

In particular, we recall the specific spaces introduced in Barrios et al. (2014). To this end, given $T \in \mathcal{T}_h$ and an integer $l \geq 0$, we denote by $\mathcal{P}_l(T)$ the space of polynomials of total degree at most l on T . Now, let $H_h \subset H(\text{div}; \Omega)$ be either the Raviart-Thomas element of order $r \geq 0$ (cf. Roberts and Thomas (1991)), i.e.

$$H_h = \mathcal{RT}_r(\mathcal{T}_h) := \{\mathbf{w}_h \in H(\text{div}; \Omega) : \mathbf{w}_{h|T} \in ([\mathcal{P}_r(T)]^d + \mathbf{x} \mathcal{P}_r(T)) \quad \forall T \in \mathcal{T}_h\}$$

where \mathbf{x} is a generic vector of \mathbb{R}^d , or the Brezzi-Douglas-Marini element of order $r + 1$, $r \geq 0$ (cf. Brezzi and Fortin (1991)), i.e.

$$H_h = \mathcal{BDM}_{r+1}(\mathcal{T}_h) := \{\mathbf{w}_h \in H(\text{div}; \Omega) : \mathbf{w}_{h|T} \in [\mathcal{P}_{r+1}(T)]^d \quad \forall T \in \mathcal{T}_h\}$$

We also recall the standard Lagrange space of order $m \geq 1$:

$$M_h := \mathcal{L}_m(\mathcal{T}_h) = \left\{ q_h \in \mathcal{C}(\bar{\Omega}) \cap L_0^2(\Omega) : q_h|_T \in \mathcal{P}_m(T), \quad \forall T \in \mathcal{T}_h \right\}.$$

The following theorem provides the rate of convergence of (6) when the specific finite element subspace is utilised.

Theorem 2.1 *Let $\kappa_1 \in (0, \frac{\alpha}{\|\mathcal{K}\|^2 \|\mathcal{K}^{-1}\|^2})$ and $\kappa_2 > 0$. Moreover, assume $\mathbf{v} \in [H^t(\Omega)]^d$, $\text{div}(\mathbf{v}) \in H^t(\Omega)$ and $p \in H^{t+1}(\Omega)$. Then, there exists $C_{\text{err}} > 0$, independent of h , such that*

$$\|(\mathbf{v} - \mathbf{v}_h, p - p_h)\|_{\mathbf{H}} \leq C_{\text{err}} h^{\min\{t, m, r+1\}} \left(\|\mathbf{v}\|_{[H^t(\Omega)]^d} + \|\text{div}(\mathbf{v})\|_{H^t(\Omega)} + \|p\|_{H^{t+1}(\Omega)} \right). \quad (7)$$

Proof. See Theorems 2.1 and 3.1 in Barrios et al. (2014). □

3 A POSTERIORI ERROR ESTIMATOR

Here we present a residual based a posteriori error estimator developed in Barrios et al. (2014). To this aim, let $(\mathbf{v}, p) \in H_\psi \times M$ and $(\mathbf{v}_h, p_h) \in (H_h \cap H_\psi) \times M_h$ be the unique solutions to problems (5) and (6), respectively.

We define the error indicator $\eta^2 := \sum_{T \in \mathcal{T}_h} \eta_T^2$, with

$$\eta_T^2 := \|\mathbf{f} - \nabla p_h - \mathcal{K}^{-1} \mathbf{v}_h\|_{[L^2(T)]^d}^2 + \|\varphi - \text{div}(\mathbf{v}_h)\|_{L^2(T)}^2.$$

The next theorem establishes the reliability and efficiency of this estimator

Theorem 3.1 *There exist a positive constant C_{rel} , independent of h , such that*

$$\|(\mathbf{v} - \mathbf{v}_h, p - p_h)\|_{\mathbf{H}} \leq C_{\text{rel}} \eta, \quad (8)$$

and there exists a positive constant C_{eff} , independent of h and T , such that

$$C_{\text{eff}} \eta_T \leq \|(\mathbf{v} - \mathbf{v}_h, p - p_h)\|_{H(\text{div}, T) \times H^1(T)}, \quad \forall T \in \mathcal{T}_h. \quad (9)$$

Proof. See Theorem 4.1 in Barrios et al. (2014). □

4 NUMERICAL EXAMPLES

In this section we present numerical results illustrating the performance of the augmented mixed finite element scheme (6) and the a posteriori error estimator η . First of all, we remark that for implementation purposes, the null media condition required to the elements of M_h is equivalent to fix the value of pressure on a point of the numerical domain.

The experiments have been performed with the finite element toolbox ALBERTA using refinement by recursive bisection (see Schmidt and Siebert (2005)), and the solution of the corresponding discrete system has been computed using the SuperLU library (see Demmel et al. (1999)).

We propose the standard adaptive finite element method (AFEM) based on the loop:

$$\text{SOLVE} \rightarrow \text{ESTIMATE} \rightarrow \text{MARK} \rightarrow \text{REFINE}.$$

Hereafter, we replace the subscript h by k , where k is the counter of the adaptive loop. Then, given a mesh \mathcal{T}_k , the procedure SOLVE is an efficient direct solver for computing the discrete

solution (\mathbf{v}_k, p_k) , ESTIMATE calculates the error indicators, $\eta_k(T)$ for all $T \in \mathcal{T}_k$ depending on the computed solution and data. Based on the values of $\{\eta_k(T)\}_{T \in \mathcal{T}_k}$, the procedure MARK generates a set of marked elements subject to refinement. For the elements selection, we rely on the *maximum* strategy: Given a threshold $\theta \in (0, 1]$, all elements $T' \in \mathcal{T}_k$ with

$$\eta_k(T') > \theta \max_{T \in \mathcal{T}_k} \eta_k(T), \quad (10)$$

are marked for refinement. In our experiments, MARK uses $\theta = 0.6$. Finally, the procedure REFINE creates a conforming refinement \mathcal{T}_{k+1} of \mathcal{T}_k , bisecting d times ($d = 2, 3$) all marked elements.

4.1 Example 1: L-shaped domain

In order to illustrate the performance of the adaptive algorithm, we take $\Omega \subset \mathbb{R}^2$ as the L-shaped domain $(-1, 1)^2 \setminus [0, 1]^2$, and we consider that the data and the exact solution (\mathbf{v}, p) of the Problem (1), in polar coordinates, are given by

$$p(r, \theta) = r^{\frac{2}{3}} \sin\left(\frac{2\theta}{3}\right) - \frac{r^2}{4}, \quad \mathcal{K} = \mathbf{I}, \quad \mathbf{f} = \mathbf{0}, \quad \mathbf{v} = -\mathcal{K} \nabla p, \quad \varphi = 1, \quad \psi = \mathbf{v} \cdot \mathbf{n}.$$

We observe that the solution of this Example is singular at the boundary point $(0, 0)$. In fact, the behaviour of p in a neighborhood of the origin implies that $p \in H^{1+2/3}(\Omega)$ only, which, according to Theorem 2.1, yields $2/3$ as the expected rate of convergence for the uniform refinement and for any conforming finite element spaces.

The values of the stabilisation parameters are chosen to be $\kappa_1 = 1.0$ and $\kappa_2 = \frac{1}{2}$, that are consistent with the theory, and ensure that the bilinear form is elliptic in the whole space. We solve Problem (6) using the finite element pair $(\mathcal{RT}_0, \mathcal{L}_1)$. In Figure 1 we provide the total errors, the theoretical rates of convergence, the a posteriori error estimators, and the effectivity indices for the uniform and adaptive refinements. We note from this figure that the errors of the adaptive procedure decrease much faster than those obtained by the uniform one; in particular, we observe approaches $2/3$ for the uniform refinement, whereas the adaptive method is able to recover, at least approximately, the quasi-optimal rate of convergence $O(h)$ for the total error. Furthermore, the effectivity indices remain again bounded from above and below, which confirms the reliability and efficiency of η for the adaptive algorithm. On the other hand, some intermediate meshes obtained with the adaptive refinement are displayed in Figures 2 and 3. Note that the method is able to recognise the singularity of the solution at the origin. The pressure and the velocity vector field are reported in Figure 4.

4.2 Example 2: Boundary layer

The aim of this example is to exhibit a numerical experiment in 3D to analyse the performance of the adaptive algorithm for an example with a boundary layer. To this end, we consider $\Omega = (0, 1)^3$ with the exact solution (\mathbf{v}, p) of (1) and the data given by

$$p(x_1, x_2, x_3) = \prod_{i=1}^3 x_i (1 - e^{(1-x_i)/\epsilon}), \quad \mathcal{K} = \epsilon \mathbf{I}, \quad \mathbf{f} = \mathbf{0}, \quad \mathbf{v} = -\mathcal{K} \nabla p, \quad \varphi = 1, \quad \psi = \mathbf{v} \cdot \mathbf{n},$$

with $\epsilon = \frac{\kappa}{\mu} = 0.05$. We observe that the solution of this example has an exponential boundary layer around the point $(1, 1, 1)$. The stabilisation parameters are chosen to be $\kappa_1 = 1.0$

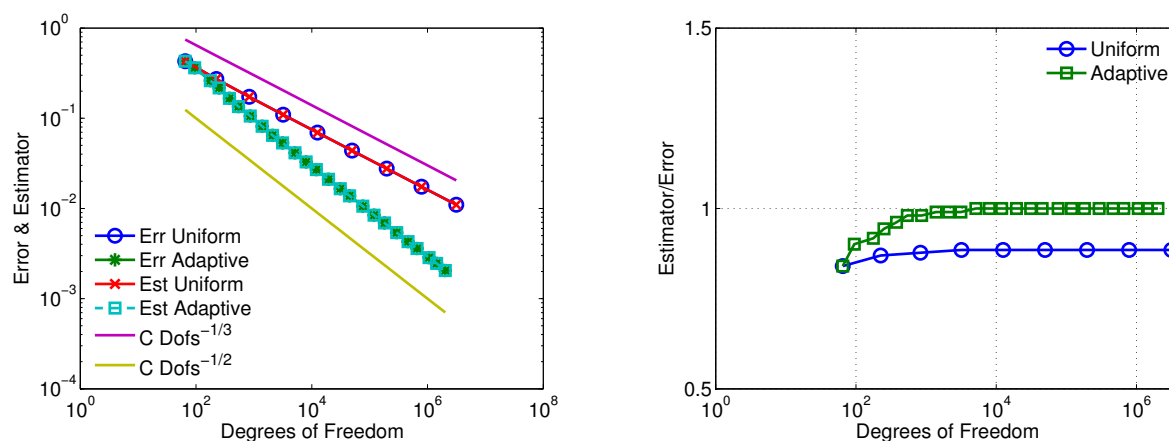


Figure 1: Example 1. Decays of total error and estimator for $(\mathcal{RT}_0, \mathcal{L}_1)$ on uniform (FEM) and adaptive (AFEM) meshes (left). Effectivity index (right).

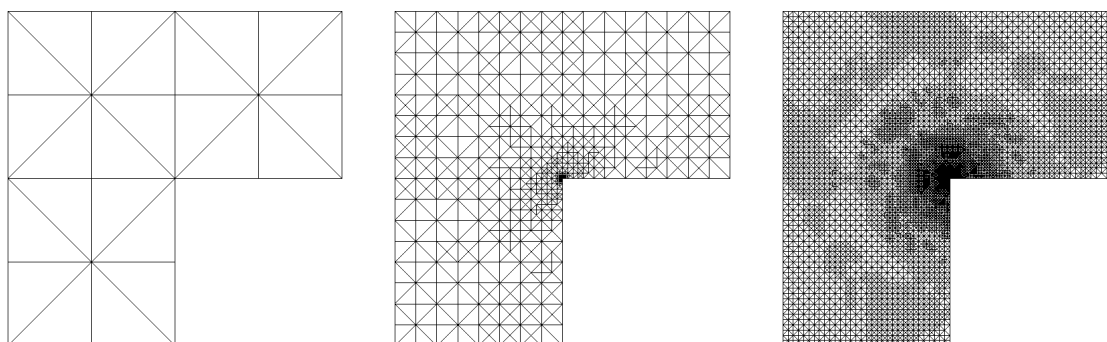


Figure 2: Example 1: Meshes after 0, 8 and 14, composed of 24, 1012 and 15362 triangles, respectively.

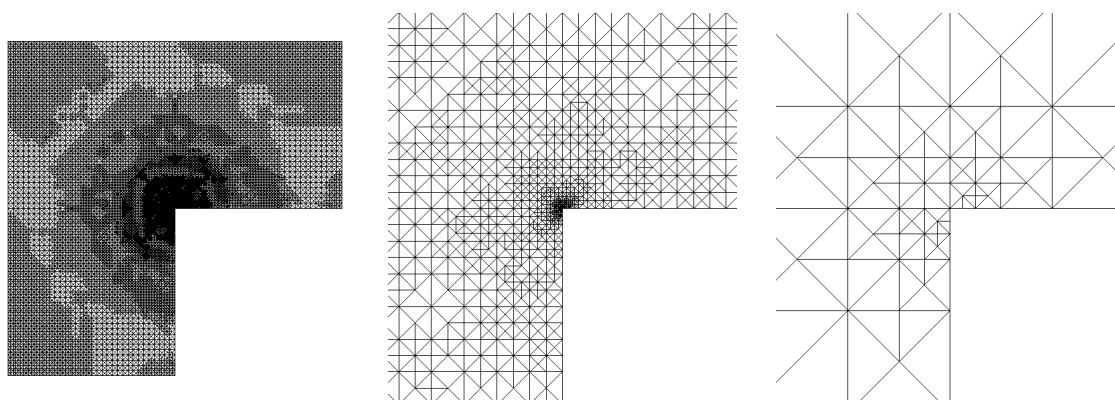


Figure 3: Example 1: Adapted mesh for 16th iteration: full mesh (left), zooms to $[10^{-2}, 10^{-2}]^2$ (center), $[10^{-4}, 10^{-4}]^2$ (right).

and $\kappa_2 = \frac{\kappa}{2\mu} = \frac{\epsilon}{2}$. In addition, we solve Problem (6) again using the finite element pair of lowest order, that is, $(\mathcal{RT}_0, \mathcal{L}_1)$. In Figure 5 we present the convergence behaviour for total errors using uniform and adaptive refinements. We note that both refinements exhibits, at least

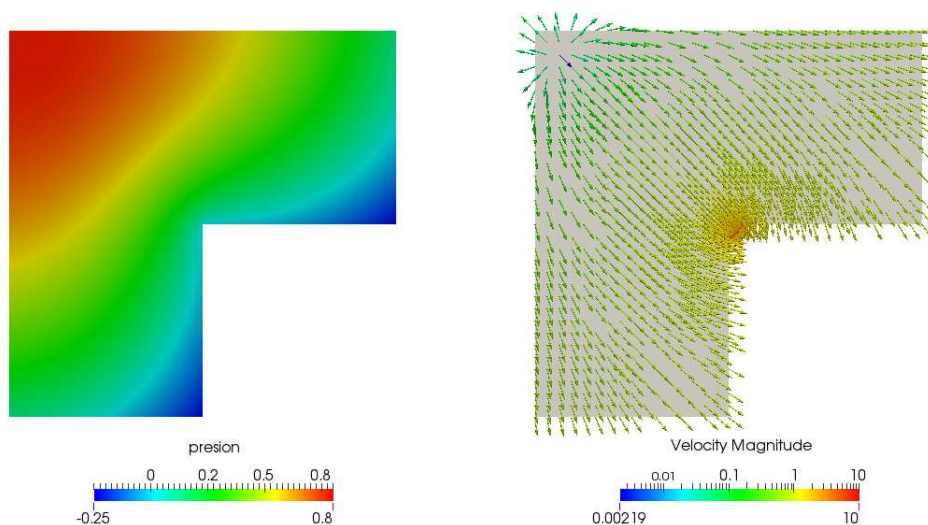


Figure 4: Example 1: Pressure (left) and vector field (right). The value of the pressure is fixed to zero in a corner of the domain. The scale is logarithmic

asymptotically, the quasi-optimal rate of convergence $O(h)$ for the total error. Furthermore, as expected, the adaptive algorithm is much faster than the uniform one, in the sense that the adaptive algorithm needs less degrees of freedom than the uniform one to obtain a given tolerance. In addition, we can see that the effectivity indexes of the a posteriori error estimator (Total error/Estimator) remain constant, which is in accordance with Theorem 3.1 .

The capability of the adaptive algorithm to localise the inner layers and/or the large stress regions of the exact solution is presented in Figures 6 and 7, where we can see the adapted meshes are refined around the point $(1, 1, 1)$. Moreover, the pressure and the velocity field has been sketched in Figure 8.

Summarizing, the numerical results presented in this section underline the reliability and efficiency of η and strongly demonstrate that the associated adaptive algorithm is much more suitable than a uniform discretization procedure when solving problems with non-smooth solutions.

ACKNOWLEDGEMENTS

This research was partially supported by Dirección de Investigación of the Universidad Católica de la Santísima Concepción, by MICINN grant MTM2010-21135-C02-01, by Secretaría de Estado de Investigación, Desarrollo e Innovación of the Ministerio de Economía y Competitividad of the Spanish Government, grant contract: CGL2011-29396-C03-02, by Consejería de Educación of the Junta de Castilla y León, Grant contract: SA266A12-2 and by CONACYT-SENER Fondo Sectorial CONACYT SENER HIDROCARBUROS, grant contract: 163723. Finally, on the occasion of the Professor Rodolfo Rodríguez's 60th birthday, the authors want to dedicate this article, expressing their gratitude for all comments/suggestions and valuable discussion through all these years.

REFERENCES

Barrios T.P., Cascón J.M., and González M. A posteriori error analysis of an augmented mixed finite element method for Darcy flow. Technical Report 2014-5, Departamento de

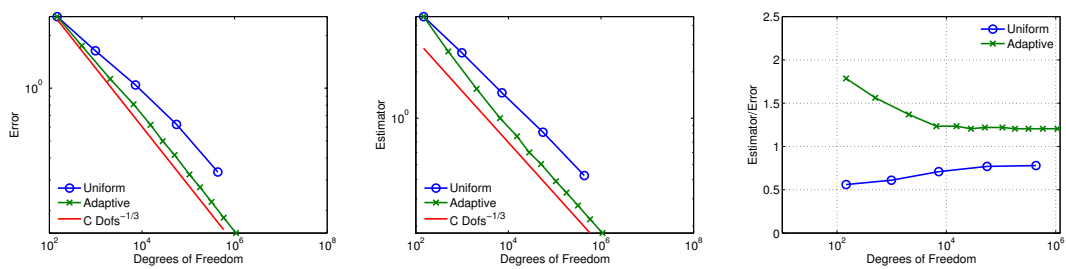


Figure 5: Example 2: Decays of total error (left) and estimator (center) for $(\mathcal{RT}_0, \mathcal{L}_1)$ on uniform (FEM) and adaptive (AFEM) meshes. Effectivity index (right)

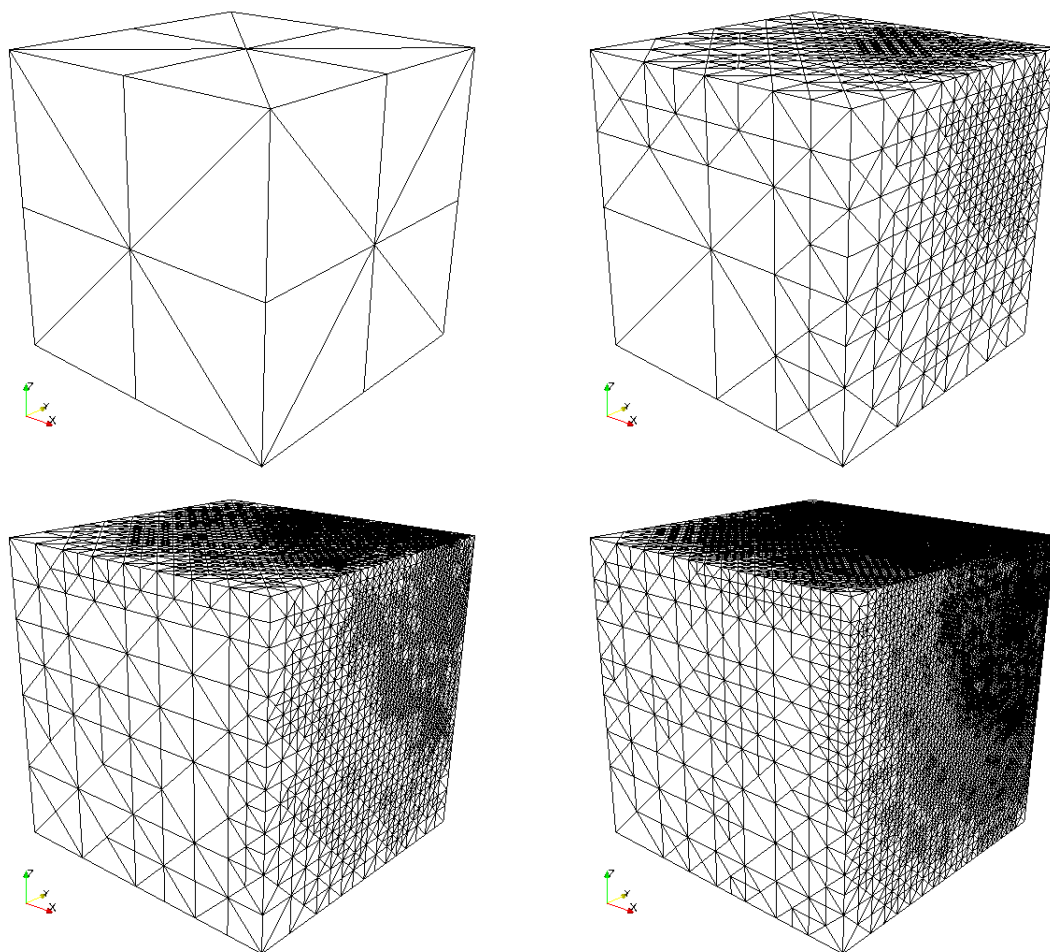


Figure 6: Example 2: Meshes after 0, 5, 8 and 16 iterations, composed of 48, 12054, 16880 and 479574 tetrahedra, respectively.

Matemática y Física Aplicadas, Universidad Católica de la Santísima Concepción, Chile, <https://dmfa.ucsc.cl/investigacion/pre-publicaciones.html>, 2014.

Barrios T.P., Gatica G.N., and Paiva F. A-priori and a-posteriori error analysis of a wavelet-based stabilization for the mixed finite element method. *Numerical Functional Analysis and Optimization*, 28:265–286, 2007.

Brezzi F. and Fortin M. *Mixed and Hybrid Finite Element Methods*, volume I. Springer, 1991.

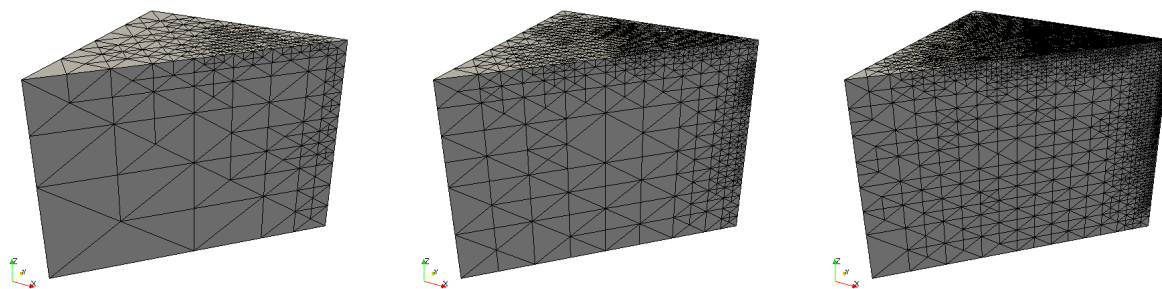


Figure 7: Example 2: Meshes after 5, 8 and 16 iterations, composed of 12054, 16880 and 479574 tetrahedra, respectively

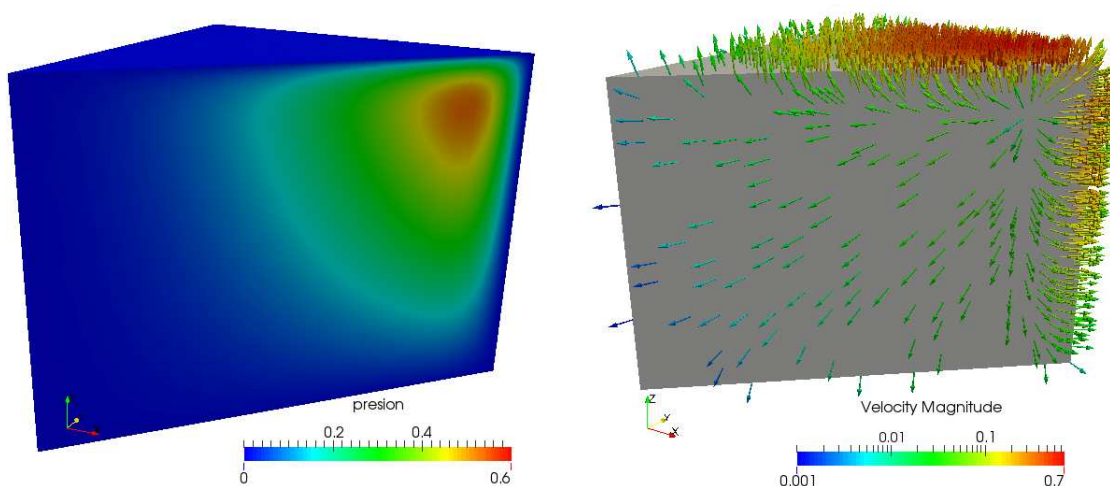


Figure 8: Example 2: Pressure and velocity field on a section of the domain $(0, 1)^3$

Demmel J.W., Eisenstat S.C., Gilbert J.R., Li X.S., and Liu J.W.H. A super nodal approach to sparse partial pivoting. *SIAM Journal of Matrix Analysis and Applications*, 20:720–755, 1999.

Larson M.G. and Malqvist A.M. A posteriori error estimates for mixed finite element approximations of elliptic problems. *Numerische Mathematik*, 108:487–500, 2008.

Masud A. and Hughes T.J.R. A stabilized mixed finite element method for Darcy flow. *Computer Methods in Applied Mechanics and Engineering*, 191:4341–4370, 2002.

Roberts J.E. and Thomas J.M. *Handbook of Numerical Analysis*, volume II, chapter Mixed and Hybrid Methods. North-Holland, 1991.

Schmidt A. and Siebert K.G. *Design of Adaptive Finite Element Software: The Finite Element Toolbox ALBERTA*, volume LNCSE 42. Springer, 2005.